วงจรกรองแถบความถี่ผ่านค่า Q สูงและวงจรออสซิลเลเตอร์แบบง่ายโดยใช้อินเวอร์เตอร์ชนิดซีมอส

Simple Configurations of Tunable High-Q Band-pass Filter and Oscillator
Based on CMOS Inverters

Vinai Silaruam[1] , Anuree Lorsawatsiri[2] and Sunee Kurutach[3]

Department of Telecommunication Engineering, Faculty of Engineering and Technology,

Mahanakorn University of Technology[1, 2, 3]

E-mail: vinai@mutacth.com[1]

บทคัดย่อ

บทความนี้นำเสนอวงจรกรองแถบความถี่ผ่านที่มีค่า Q สูงและวงจรออสซิลเลเตอร์โดยใช้ตัวอินเวอร์เตอร์และตัวเก็บประจุต่อร่วมกัน โดยวงจรที่นำเสนอมีข้อดี คือ มีโครงสร้างเรียบง่ายที่ปราศจากตัวต้านทานและใช้จำนวนอุปกรณ์ในแต่ละวงจรน้อย รวมถึงเหมาะกับการใช้งานในระบบที่มีไฟเลี้ยงต่ำ นอกจากนี้ ยังปรับรูปแบบของวงจรเป็นแบบสมดุลได้ ผลการจำลองการทำงานของวงจรที่นำเสนอซึ่งใช้เทคโนโลยีชนิดซีมอส 0.18 μm ยังยืนยันความเป็นไปได้และสมรรถนะของวงจรด้วย

Abstract

Simple tunable high-Q band-pass filters and oscillators based on inverter-C are presented. Advantageous features of the proposed circuits include circuit simplicity, resistorless topologies and offer, at present, the lowest component count. These circuits are simply obtained by a slight modification of a conventional inverter-C filter. Owing to simple structures, the circuits are also suitable for low power supply systems. Furthermore, the principle is extended to include fully balanced versions of these circuits. Simulation results of the circuit design on 0.18μm CMOS process are demonstrated to confirm the validity and circuit performances.

1. Introduction

Band-pass filters and oscillators find a wide range of applications in telecommunications, control systems, signal processing and measurement systems. In designing band-pass filters and sinusoidal oscillators, varieties of circuitry have been reported [1 - 2]. However, some of them are meant to operate neither at high frequencies nor low-voltage supplies. Recently, several popular circuits based on g_m-C and gyrator-C topologies, which suitable for high-frequency applications, are presented [3 - 5]. The digitally used CMOS inverters realize analog operator, i.e. transconductors suiting low-voltage operation. In

particular, the operation reaches the extreme for the analog part, since there are only two transistors stacked in between supply rails. The concept of using CMOS inverters to implement analog transconductors is given in [6 - 7].

According to the technology available today, mixed analog and digital circuits are implemented on the same integrated circuit (IC) chip. Therefore, a fully balanced architecture is preferable for analog implementation, as fully balanced systems are more immune to digital noise. Besides, fully balanced architecture is used in high performance analog applications to enhance the dynamic range, reduce harmonic distortion, and minimize the effect from coupling among various blocks [8].

In this work, simple forms of tunable high-Q band-pass filters and oscillators employing inverter-C based on a passive RC filter are presented. Basic transimpedance (current-to-voltage) RC filter topologies are first described. Next, an inverter-C filter is generated with CMOS inverters employed as resistors. With the feedback technique, the filter can easily be modified to obtain a tunable band-pass filter and a tunable oscillator. Then they are further arranged to be in fully balanced forms. Moreover, utilizing parasitic capacitances of the inverters as grounded capacitances, the circuitry possesses minimum components. Finally to confirm the validity and performances of the proposed work, numerous simulations are demonstrated.

2. Overview of the CMOS Inverters

In this work, as the CMOS inverter is mainly used as an active cell in transconductance mode, the related principle is essentially reviewed. The CMOS inverter is widely used in digital signal processing. Normally an inverter reaches an equilibrium (choosing $L_N = L_P$) around $W_P = (\mu_N / \mu_P)W_N$, where W_N and W_P (L_N and L_P) are the channel width (channel length) and μ_N and μ_P are the carrier mobility of NMOS and PMOS transistors, respectively. Figure 1(a) shows the typical CMOS inverter and Figure 1(b) its universal symbol. In digital mode of operation with node OUT open, these transistors both work in saturation around this particular operating point [8 - 9]. In the transconductance mode of operation, a small signal v_{in} is applied around the DC common mode voltage ($V_{CM} = V_{DD} / 2$). In response to small signal amplitude, the CMOS inverter develops a transconductor between the input voltage (v_{in}) and the output current (i_{out}) (see Figure 1(c)). At low-frequency, the small-signal output current of the inverter in the transconductance mode is given by

$$i_{out} = -g_m v_{in} \tag{1}$$

where $g_m = (g_{mN} + g_{mP})$. The inverter transconductance g_m is around the common mode voltage (V_{CM}) and g_{mN} and g_{mP} are, respectively, the NMOS and PMOS gate-source transconductances in saturation mode [10]. Because in general both inverting and non-inverting transconductance is needed, a suitable realization and symbolic representation, using the circuit of Figure 1(a) are shown in Figure 1(d) and (e).
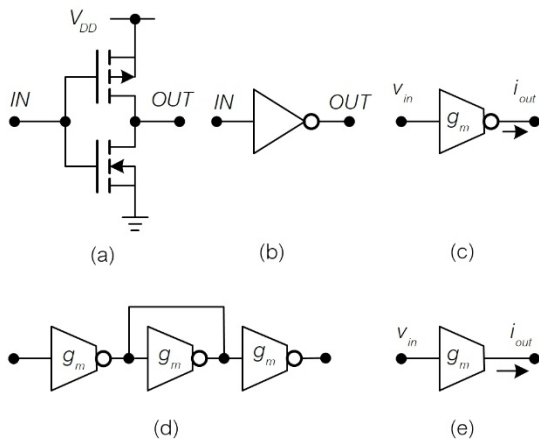

(a)   (b)   (c)

(d)   (e)

Fig. 1 CMOS inverter (a) circuit configuration,

(b) universal symbol, (c) inverting symbol,

(d) non-inverting transconductance operation,

(e) non-inverting symbol.

It is worth noting that when the circuit with a single power supply as shown in Figure 1(a) is replaced with having a dual power supply as shown in Figure 2(a), the common mode voltage V_{CM} of an inverter can be shifted to the ground level. Therefore, it is simply more attractive to employ the dual power supply system and so does this presented work.
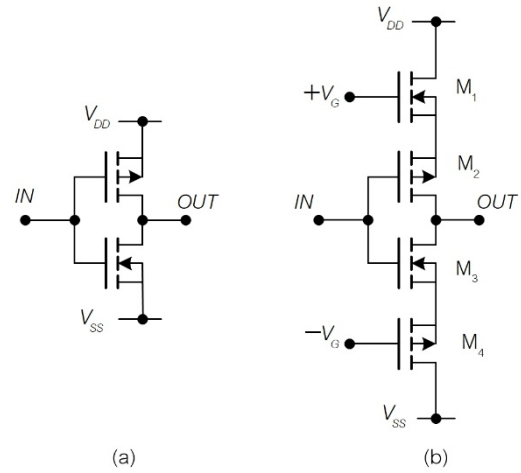

(a)   (b)

Fig. 2 (a) Dual power supply inverter,

(b) Tunable inverting transconductor.

Then two-transistor inverter in Figure 2 is easily modified to obtain a tunable transconductor, illustrated in Figure 2(b). The transconductance realized by the circuit is

$$g_m = \frac{2k_N k_P}{(\sqrt{k_N} + \sqrt{k_P})^2}\left[2V_G - \sum V_T\right] \qquad (2)$$

where

$$k_{N,P} = 0.5[\mu C_{ox} W / L]_{N,P}$$

(3)

$$\sum V_T = V_{TN1} + V_{TN3} + \left|V_{TP2}\right| + \left|V_{TP4}\right| \qquad (4)$$

and V_{TN1}, V_{TN3}, V_{TP2} and V_{TP4} are the threshold voltages of the NMOS and PMOS transistors and C_{ox} is the oxide capacitance in structure of MOS transistor [11]. The electronic tunability of this four-transistor inverter is possible by conveniently adjusting the bias voltage V_G.

3. Configuration and Analysis of the Proposed Circuits

3.1 Single-ended Band-pass Filter

For classification of what to follow, a simple RC filter in Figure 3(a) is first described. Routine analysis yields the current-to-voltage relationship, i.e. the transimpedance transfer function as follows

$$A_1(s) = \frac{sC_3}{s^2 C_T + s(\frac{C_a}{R_1} + \frac{C_b}{R_1}) + \frac{1}{R_1 R_2}} \qquad (5)$$

where $C_T = C_1 C_3 + C_2 C_3 + C_1 C_2$, $C_a = C_2 + C_3$, $C_b = C_1 + C_3$. Utilizing transconductors in place of all resistors, the transfer function in (5) becomes

$$A_2(s) = \frac{sC_3}{s^2 C_T + s(g_{m1} C_a + g_{m2} C_b) + g_{m1} g_{m2}} \qquad (6)$$

where g_{m1} and g_{m2} are the transconductances of the T_1 and T_1 transconductors, respectively. This results in another circuit configuration in the form of the g_m-C filter illustrated in Figure 3(b). The transfer function in (6) is the characteristic of the band-pass filter (BPF) with a center frequency,

$$f_0 = \frac{1}{2\pi} \sqrt{\frac{g_{m1} g_{m2}}{C_T}} \qquad (7)$$

and a quality factor,

$$Q = \frac{\sqrt{g_{m1} g_{m2} C_T}}{g_{m1} C_a + g_{m2} C_b} \qquad (8)$$
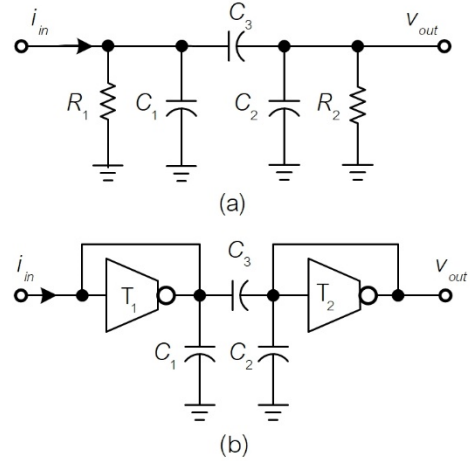

(a)

(b)

Fig. 3 Basic band-pass filters;

(a) RC filter, (b) g_m-C filter.

Given a center frequency f_0, then it is hard if not impossible to tune the quality factor Q by adjusting the filter parameters via iteration process. To get over this drawback, a slight modification is made to the BPF in Figure 3(b). Employing one transconductor to feed the output back to the input node, as shown in Figure 4, results in a tunable single-ended transimpedance BPF.
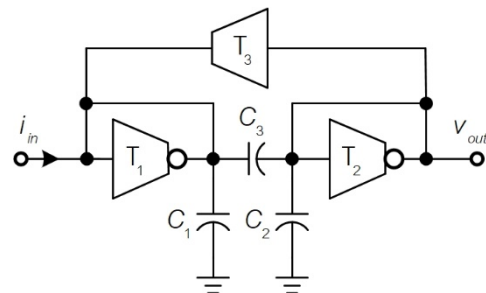

Fig. 4 Proposed single-ended transimpedance BPF.

A simple analysis of Figure 4 gives the following I-V transfer function

$$A_3(s) = \frac{sC_3}{s^2 C_T + s(g_{m1}C_a + g_{m2}C_b - g_{m3}C_3) + g_{m1}g_{m2}} \quad (9)$$

The center frequency of the filter is given in (7) and the quality factor of the filter is,

$$Q = \frac{\sqrt{g_{m1}g_{m2}C_T}}{g_{m1}C_a + g_{m2}C_b - g_{m3}C_3} \quad (10)$$

Note that, the maximum magnitude of the transfer function given in (9) is

$$A_0 = \frac{C_3}{g_{m1}C_a + g_{m2}C_b - g_{m3}C_3} \quad (11)$$

Remarkably, the quality factor Q given in (10) is independent from the center frequency of the filter f_0 given in (7). The former can be freely varied by adjusting the transconductance g_{m3}. Moreover, the parasitic capacitors at the input and output nodes of the proposed BPF can be lumped in place of C_1 and C_2, respectively. As a result, the circuit can be operated at a very high frequency with the minimum component count.

The circuit construction of the filter in Figure 4 can be easily converted to a BPF with a current-mode or voltage-mode transfer function. It is possible by simply connecting the filter in Figure 4 with a T_4 transconductor at the output node for the current-mode or input node for the voltage-mode, resulting in the circuit configuration as shown in Figure 5(a) and (b), respectively.
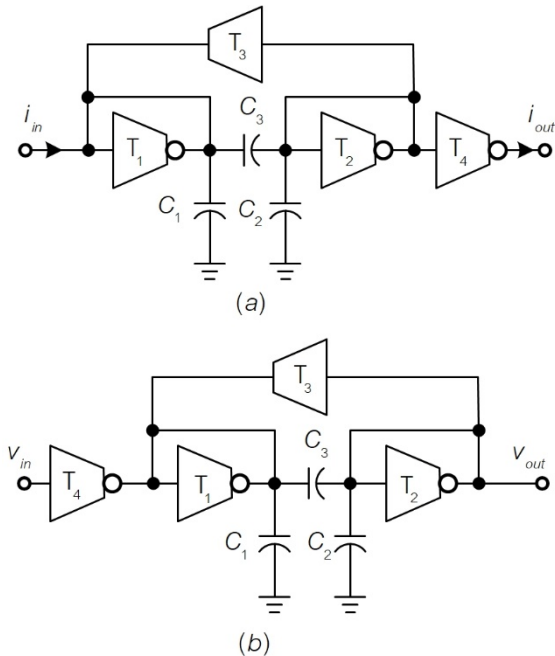

(a)

(b)

Fig. 5 Modified single-ended transimpedance BP (a) current-mode, (b) voltage-mode.

The current and voltage transfer functions of the filters in Figure 5(a) and (b) are then found to be in the same pattern as follows

$$A_4(s) = \frac{sg_{m4}C_3}{s^2 C_T + s(g_{m1}C_a + g_{m2}C_b - g_{m3}C_3) + g_{m1}g_{m2}} \quad (12)$$

Note that the simple structure of the inverter makes it attractive for both very high frequency and low-voltage operations.

3.2 Fully-balanced Band-pass Filter

There are several methods to implement the BPF in Figure 4 depending on the type of the

transconductors. If all transconductors are implemented by the inverter as shown in Figure 2(a), the fully-balanced BPF can be further realized quite easily. Such one is shown in Figure 6.
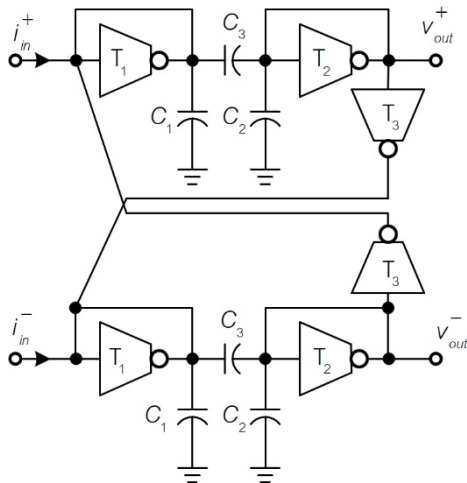

Fig. 6 Proposed fully-balanced transimpedance BPF.

From Figure 6, it is noticed that the balanced BPF in current-mode or voltage-mode transfer functions can be realized by simply connecting a transconductor to, respectively, the output or the input node of the filter. This is carried out just in the same manner as in the case of the single-ended BPF in Figure 5.

Last but not least, these proposed filters can be reconstructed to obtain the electronic tunability feature. It is carried out by simply employing the transconductor of Figure 2(b) in place of the two-transistor inverter. Then the center frequencies of the filters can be adjusted through g_{m1} and g_{m2} and the quality factors of the filters can be independently adjusted via g_{m3}.

3.3 BPF-based Oscillators

It should be noted that the filter in Figure 4 and Figure 6 can be correspondingly modified to oscillators very easily. To start the oscillation, the feedback through the transconductors g_{m3} should be large enough to place the poles of the filters at the right half-plane. Therefore, the minimum requirement for g_{m3} is given by

$$g_{m3} \geq \frac{g_{m1}C_a + g_{m2}C_b}{C_3} \qquad (13)$$

The oscillation frequency is set by the BPF center frequency in (7). Note that if capacitors and transconductors are chosen as $C_1 = C_2$ and $g_{m1} = g_{m2}$ for design convenience, then

$$f_0 = \frac{1}{2\pi} \frac{g_{m1}}{\sqrt{C_1(2C_3 + C_1)}} \qquad (14)$$

and

$$g_{m3\min} = 2g_{m1}(1 + \frac{C_1}{C_3}) \qquad (15)$$

The frequency of oscillation can be varied by adjusting the transconductance g_{m1}. Therefore, the proposed circuit can also be used as a voltage-controlled oscillator (VCO) by utilizing a four-transistor tunable transconductor (inverter) in Figure 2(b) to replace the traditional two-transistor inverter.

4. Simulation Results

The performances of the proposed BPF and oscillator are verified by the SPICE simulation. The circuits have been simulated using BSIM3 version 3.1 SPICE model for a TSMC 0.18μm CMOS process available from MOSIS with a supply voltage of 1.8V [12].

Consider first the proposed single-ended and fully-balanced BPFs of Figure 4 and Figure 6 using a two-transistor inverter (Figure 2(a)) as an inverting transconductor. They were designed for an ideal center frequency of f_0 = 76.92 MHz and a quality factor of Q = 50. From (7) and (10), select the filter components as follows: $C_1 = C_2$ = 2 pF, C_3 = 8 pF, $g_{m1} = g_{m2}$ = 2.90 mA/V, and g_{m3} = 7.20 mA/V. The transcondcutances result from the transistor dimension as shown in Table 1.

Table 1 Aspect ratios of the MOS transistors.

Transconductors	L_N and L_P (μm)	W_N (μm)	W_P (μm)
T_1 and T_2	0.36	3.60	10.80
T_3	0.36	10.08	30.24

Figure 7 shows the simulated frequency response of the filters. The dashed and solid lines represent the response of the single-ended and fully-balanced BPFs, respectively. The quality factor of the single-ended BPF was 40 at the center frequency of 75.62 MHz and the quality factor of the fully-balanced filter was 42 at the

center frequency of 76.21 MHz. Consistently with (13), setting transconductance g_{m3} to 7.89 mA/V with L_N.= L_P = 0.36 μm, W_N = 10.8 μm and W_P = 32.4 μm. The proposed filters are easily modified to the oscillators. Figure 8 and Figure 9 show the simulated transient responses of the single-ended and fully-balanced oscillators, respectively. The oscillation frequencies of both oscillators are the same as the center frequencies of the proposed BPFs.
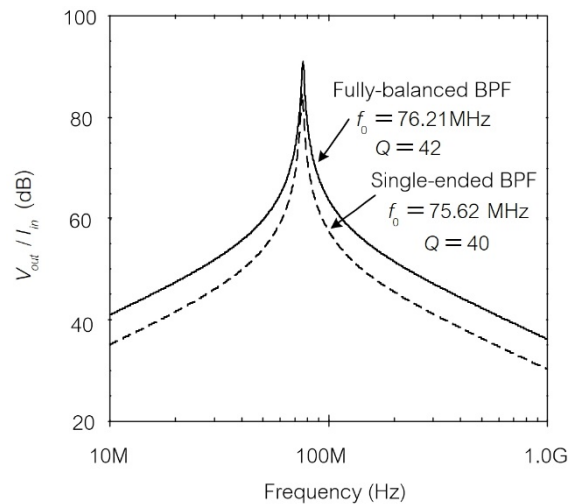

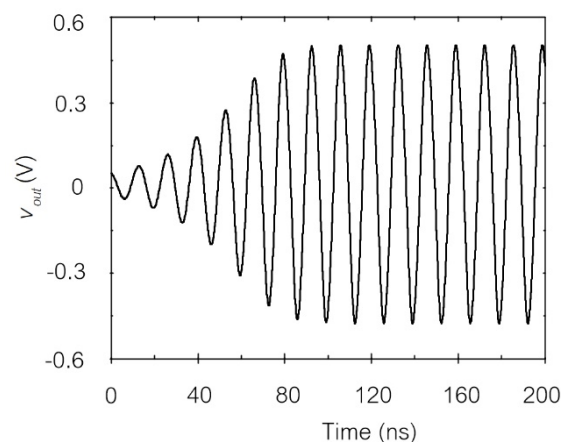Fig. 7 Frequency responses of the proposed BPFs.

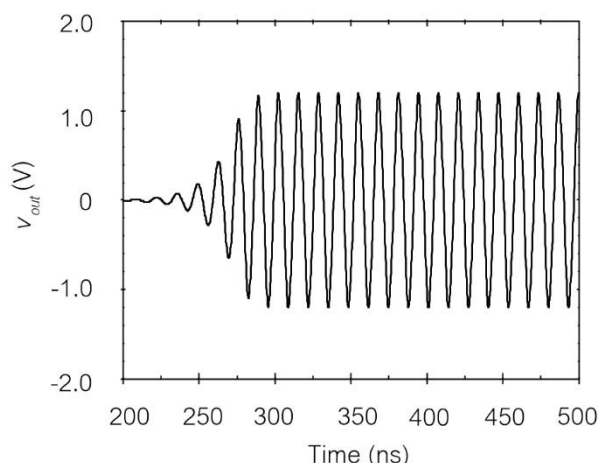Fig. 8 Transient response of the single-ended oscillator.

Fig. 9 Transient response of the fully-balanced oscillator.

The spectrum of the sinusoidal output of Figure 8 is shown in Figure 10. The total harmonic distortion (THD) is around 0.19 %.
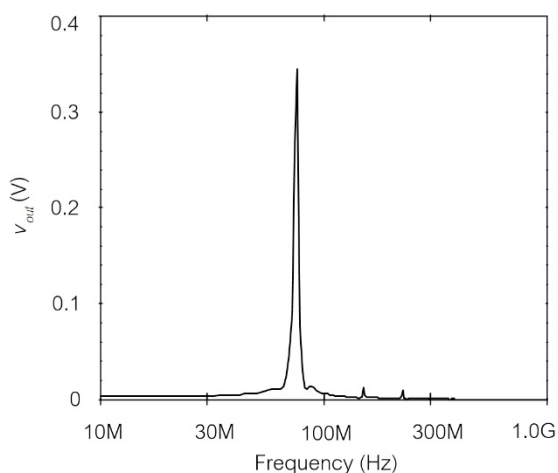

Fig. 10 Spectrum of signal in Figure 8.

Then, the proposed single-ended oscillator can be operated at very high frequency by using the parasitic capacitors at the input and output nodes of the circuit as C_1 and C_2, respectively. Figure 11 shows the transient response of the single-ended oscillator when C_3

= 0.7 pF, using the transistor dimensions of the transconductors T_1 and T_2 as shown in table 1, setting $L_N = L_P = 0.36$ μm, $W_N = 10.8$ μm, and W_P = 32.4 μm for transconductor T_3, parasitic input capacitor C_1 = 108 fF, and parasitic output capacitor C_2 = 37 fF [13]. From the figure, the oscillation frequency of the sinusoidal output signal was 700 MHz.
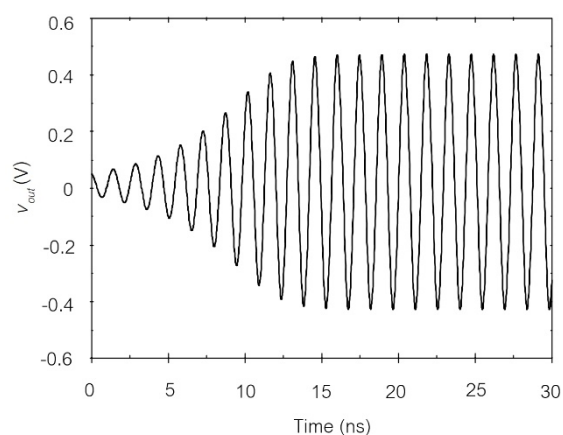

Fig. 11 Transient response of the single-ended oscillator using parasitic capacitors.

In order to demonstrate the electronic tunability of the proposed BPF and oscillator with four-transistor transconductor (Figure 2(b)), these circuit components are selected $C_1 = C_2 = 1$ pF, $C_3 = 3.5$ pF and dimension transistors as $L_N = L_P$ = 0.36 μm for all transistors, $W_N = 7.2$ μm and W_P = 21.6 μm for transconductor T_1 and T_2 , $W_N =$ 21.6 μm and $W_P = 64.8$ μm for transconductor T_3 are selected. The quality factor tuning of the single-ended BPF with center frequency of 72 MHz is shown in Figure 12. The quality factors were 146.94, 19.73 and 10.56 when the bias

voltage of the transconductor T_3, $\pm V_{G3} = 1.68$ V, 1.70 V, and 1.72 V, respectively.
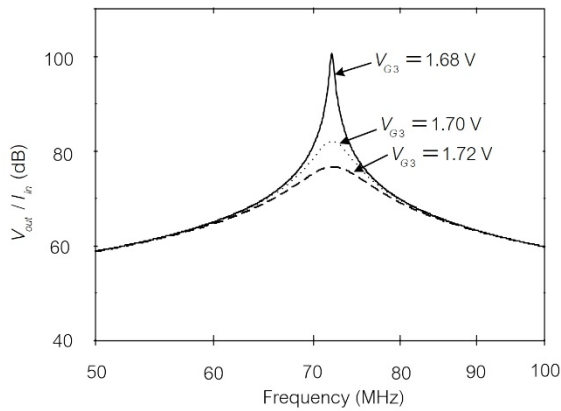

Fig. 12 Quality factor tuning of the single-ended BPF.

Figure 13 shows the simulated output waveform of the single-ended oscillator with $\pm V_{G1} = \pm V_{G2} = 1.7$ V and $\pm V_{G3} = 1.8$ V. Figure 14 displays the oscillation frequency of the oscillator versus $\pm V_{G1}$, the oscillation frequency varies from 50 MHz to 75MHz when $\pm V_{G1}$ adjusts from 1 V to 1.7 V.
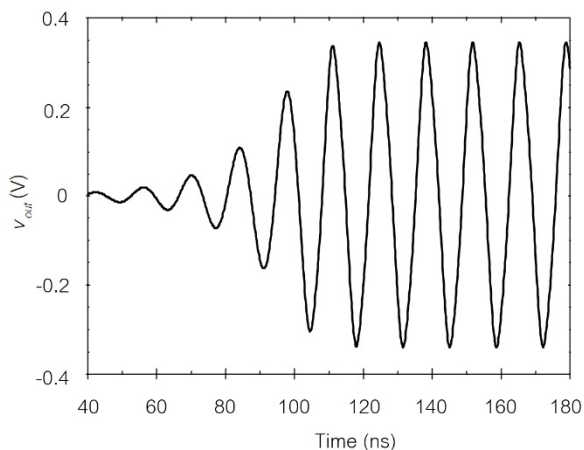

Fig. 13 Transient response of the single-ended oscillator with $\pm V_{G1} = \pm V_{G2} = 1.7$ V , $\pm V_{G3} = 1.8$ V.
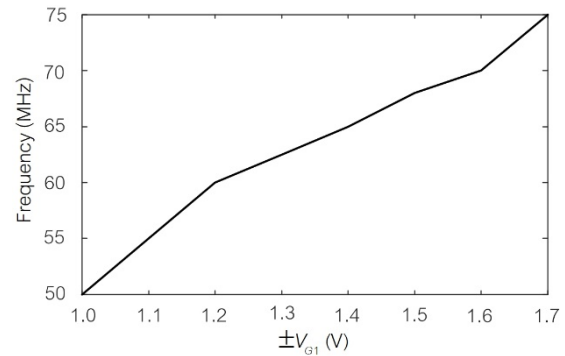

Fig. 14 Oscillation frequency of the single-ended oscillator by adjusting $\pm V_{G1}$.

Finally, Figure 15 shows the oscillation frequency of the oscillator versus g_{m1}, resulting in a graph almost identical to a linear relation of both parameters.
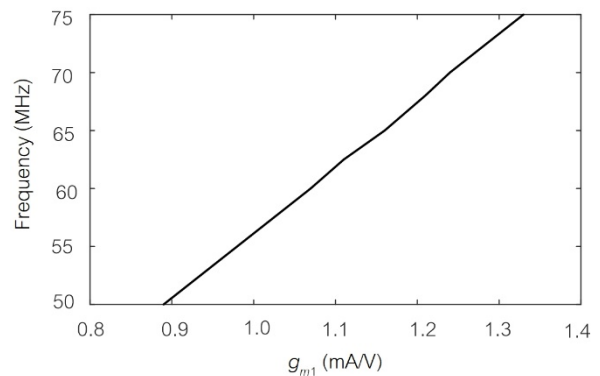

Fig. 15 Oscillation frequency of the single-ended oscillator versus g_{m1} tunning.

5. Conclusion

Simple configurations of new tunable high-Q band-pass filters and oscillators have been proposed. These circuits are obtained from the modification of the transimpedance inverter-C filter with the feedback technique. The attractive features of the circuit include suitable for low

power supply, simple structure, and low component count. Moreover, the electronic tunability of the quality factor, frequency center, and oscillation frequency can be obtained by adjusting the bias voltage of the inverter. The simulation results have been shown that the quality factor Q can be as high as 146.94 with center frequency $f_0 = 72$ MHz for the band-pass filter and the oscillation frequency of oscillator can be tuned up to 700 MHz.

Acknowledgements

References

[1] Keskin, A. U. "Voltage-mode high-Q band-pass filters and oscillators employing single CDBA and minimum number of component", International Journal of Electronics, 2005, vol. 92, no. 8, p. 479 - 487.

[2] Kumar, S., Govil, A., Bhattacharyya, A. and Dutta, D. "A wide-range tunable bandpass filter cum sinusoidal oscillator using a new current-controlled resistor", In Proceedings of the 1999 IEEE International Symposium on Circuit and Systems. Orlando (United States), 1999, p. 220 – 223.

[3] Kumar, U. "Simulation and realization of some CMOS transconductor VHF filters", Active and Passive Electronic Components, 2003, vol. 26, no. 3, p. 133 – 136.

[4] Chang, C. M. "Novel current conveyor based single resistance controlled voltage controlled oscillator employing grounded resistors and capacitors", Electronics Letters, 1994, vol. 30, no. 3, p. 181 – 183.

[5] Liu, S. I. "Single resistance controlled/voltage controlled oscillator using current conveyors and grounded capacitors", Electronics Letters, 1995, vol. 31, no. 5, p. 337 – 338.

[6] Khan, A. A., Bimal, S., Dey, K. K. and Roy, S. S. "Novel RC sinusoidal oscillator using second generation current conveyor", IEEE Transactions on Instrumentation and Measurement, 2005, vol. 54, no. 6, p. 2402 – 2406.

[7] Horng, J. W., Chang, C. W. and Lee, M. H. "Single element controlled sinusoidal oscillators using CCIIs" International Journal of Electronics, 1997, vol. 83, no. 6, p. 831 – 836.

[8] Thanachayanont, A. "Low-voltage low-power high-Q CMOS RF bandpass filter", Electronics Letters, 2002, vol. 38, no. 13, p. 615 – 616.

[9] Wu, Y., Shi, C., Ding, X., Ismail, M. and Olsson, H. "Design of CMOS VHF/RF biquadratic filters", Analog Integrated Circuits and Signal Processing, 2002, vol. 33, no. 3, p. 239 – 248.

[10] Andreani, P. and Mattisson, S. "On the use of Nauta's transconductor in low-frequency CMOS gm-C bandpass filter", IEEE Journal of Solid-state Circuits, 2002, vol. 37, no. 2, p. 114 – 124.

[11] Nauta, B. and Seevinck, E. "Linear CMOS transconductance element for VHF filters", Electronics Letters, 1989, vol.25, no. 7, p. 448 – 450.

[12] Nauta, B. "A CMOS transconductance-C filter technique for very high frequencies", IEEE Journal of Solid-state Circuits, 1992, vol. 27, no. 2, p. 143 – 153.

[13] Geiger, R. L., Allen, P. E. and Strader, N. "VLSI design techniques for analog and digital circuits", New York: Mc Grall Hill, 1990.

[14] Barker, R. J., Li, H. W. and Boyce, D. E. "CMOS circuit design, layout, and simulation", New York: John Wiley & Sons, 1990.

[15] Barthelemy, H., Meillere, S., Gaubert, J., Dehaese, N. and Bourdel, S. "OTA based on CMOS inverters and application in design of tunable bandpass filter", Analog Integrated Circuits and Signal Processing, 2008, vol. 57, no. 3, p. 169 – 178.

[16] Park, C. S. and Schaumann, R. "A high frequency CMOS linear transconductance element", IEEE Transactions on Circuits and Systems, 1986, vol. CAS – 33, no. 11, p. 1132 – 1138.

[17] The MOSIS Service, USA. Wafer electrical test data and SPICE model parameter. 4 pages. [Online] Cited 2012-01-31. Available at: http://www.mosis.org/test/.

[18] Laker, K. R. and Sansen, W. M. C. "Design of analog integrated circuits and systems", Singapore: Mc Grall Hill, 1994.

About Authors

Vinai SILARUAM was born in Khonkaen, Thailand. He received his B. Eng., M. Eng. and D. Eng. degrees from King Mongkut's Institute of Technology Ladkrabang (KMITL), Bangkok, Thailand, in 1993, 2000 and 2014, respectively. In 1996, he joined the Faculty of Engineering and Technology at the Mahanakorn University of Technology. His research interests include analog circuit design, analog and digital signal processing, embedded system applications and internet of things applications.

Anuree LORSAWATSIRI was born in Chiangrai, Thailand. She received the B. Eng., M. Eng. and D. Eng. degrees from King Mongkut's Institute of

Technology Ladkrabang (KMITL), Bangkok, Thailand, in 1997, 2001 and 2014, respectively. In 1997, she joined the Faculty of Engineering and Technology at the Mahanakorn University of Technology where she is employed as a lecturer. Her main research interests are in the areas of analog and digital communications and circuit theory.

Sunee KURUTACH received her B. Eng. degree from King Mongkut's Institute of Technology Ladkrabang (KMITL), Bangkok, Thailand, in 1988 and M. EngSc degree from The University of New South Wales, Australia, in 1990. In 1996, she joined the Faculty of Engineering and Technology at Mahanakorn University of Technology as a lecturer. Her main research interest is in the area of Electromagnetic.